

Analysis of a damaged industrial hall subjected to the effects of fire

Stanislav Kmet^{*1}, Michal Tomko^{1a}, Ivo Demjan^{1b}, Ladislav Pesek^{2c}
and Sergej Priganc^{1d}

¹*Institute of Structural Engineering, Faculty of Civil Engineering, Technical University of Kosice,
Vysokoskolska 4, Kosice, Slovakia*

²*Department of Material Science, Faculty of Metallurgy, Technical University of Kosice,
Park Komenskeho 11, Kosice, Slovakia*

(Received December 12, 2015, Revised February 3, 2016, Accepted February 19, 2016)

Abstract. The results of diagnostics and analysis of an industrial hall located on the premises of a thermal power plant severely damaged by fire are presented in the paper. The comprehensive failure-related diagnostics, non-destructive and destructive tests of steel and concrete materials, geodetic surveying of selected structural members, numerical modelling, static analysis and reliability assessment were focused on two basic goals: The determination of the current technical condition of the load bearing structure and the assessment of its post fire resistance as well as assessing the degree of damage and subsequent design of reconstruction measures and arrangements which would enable the safe and reliable use of the building. The current mechanical properties of the steel material obtained from the tests and measured geometric characteristics of the structural members with imperfections were employed in finite element models to study the post-fire behaviour of the structure. In order to compare the behaviour of the numerically modelled steel roof truss, subjected to the effects of fire, with the real post-fire response of the damaged structure theoretically obtained resistance, critical temperature and the time at which the structure no longer meets the required reliability criteria under its given loading are compared with real values. A very good agreement between the simulated results and real characteristics of the structure after the fire was observed.

Keywords: damaged industrial hall; fire effects; failure diagnostics; non-destructive and destructive tests; geodetic surveying; finite element analysis; reliability assessment; fire resistance check

1. Introduction

It is well known that fire can cause severe damage to steel structures. There are documented cases of fires that have directly led to the collapse of structures or significant failures of bearing

*Corresponding author, Professor, E-mail: stanislav.kmet@tuke.sk

^aAssociate Professor, E-mail: michal.tomko@tuke.sk

^bPh.D., E-mail: ivo.demjan@tuke.sk

^cProfessor, E-mail: ladislav.pesek@tuke.sk

^dAssociate Professor, E-mail: sergej.priganc@tuke.sk

systems. In such cases the structures usually require extensive repair or complete rebuilding. However, if the damage is less severe, the effects and consequences of the fire are unclear (Brandt *et al.* 2011). In these cases a post-fire inspection and evaluation of structures must be conducted in order to analyse potential causes of failure, the actual extent of the damage and its consequences. Evaluation techniques that can be performed easily in the field, but still uniform and meaningful information for this situation are lacking.

However, the prudent determination of suitability for reuse or rehabilitation of fire-damaged steel structure requires a post-fire structural evaluation, which can be greatly aided through the application of testing for a quantitative assessment of residual material properties, structural resistance, and serviceability (Whelan *et al.* 2005).

Identifying research and development needs for large-scale experiments of fire resistance of structures are needed to support performance-based engineering and structure-fire model validation. The past two decades have seen significant advances in the understanding of the behaviour of steel subjected to fire, and it can now justifiably be claimed that more is known about steel than any other framing material in fire. Rigorous testing, both small and large scale, has led to the development of modelling and analytical techniques that are being constantly improved by some of the leading universities and research centres. Full-scale fire tests of structures were performed by several authors (Bailey 2004, Wald *et al.* 2006, Foster *et al.* 2007, Wald *et al.* 2009).

Jin *et al.* (2011) presented experimental and numerical results of the mechanical behaviour of steel planar tubular truss which was exposed to fire conditions. Chen and Zhang (2011) experimentally studied the mechanical behaviour and failure mode of a steel staggered truss system under pool fire conditions. Ho *et al.* (2011) presented a structural fire engineering study on the thermal and structural performance of unprotected long span steel trusses. Ozyurt and Wang (2015) presented the results of a numerical investigation into the behaviour of welded steel tubular truss members exposed to uniform fire. He *et al.* (2013) focused on studying the fire resistance and failure mode of circular hollow section (CHS) tubular K-joints at elevated temperature under brace axial loading at the brace ends. Gunalan and Mahendran (2014) presented a detailed experimental study of the post-fire mechanical properties of cold-formed steels. Olmati *et al.* (2013) proposed robust numerical procedures for the structural assessment of steel buildings under explosions. JalaliLarijani *et al.* (2013) assessed the vulnerability of two existing asymmetric steel building frames to progressive collapse using a linear static procedure. Krentowski (2015) scrutinized a disaster of an industrial hall caused by an explosion of wood dust and fire.

Reinforced concrete structures are vulnerable to high temperature conditions such as those during a fire. At elevated temperatures, the mechanical properties of concrete and reinforcing steel as well as the bond between steel rebar and concrete may significantly deteriorate. Aslani and Bastami (2011) developed constitutive relationships for normal-strength concrete and high-strength concrete subjected to fire to provide efficient modelling and specify the fire-performance criteria for concrete structures exposed to fire. Aslani and Samali (2013) developed bond constitutive relationships for normal and high-strength concrete subjected to fire. Choi *et al.* (2012) proposed a nonlinear computational modelling approach for the behaviours of structural systems subjected to fire.

However, research of structures and materials subjected to the effects of fire is mostly orientated to experimental and theoretical comparative studies of behaviour in fire conditions. Complex studies on a post-fire inspection, evaluation and analysis of structures, as presented in this paper, are rare.

The basic motivation for this study was to contribute to the development of methodology and

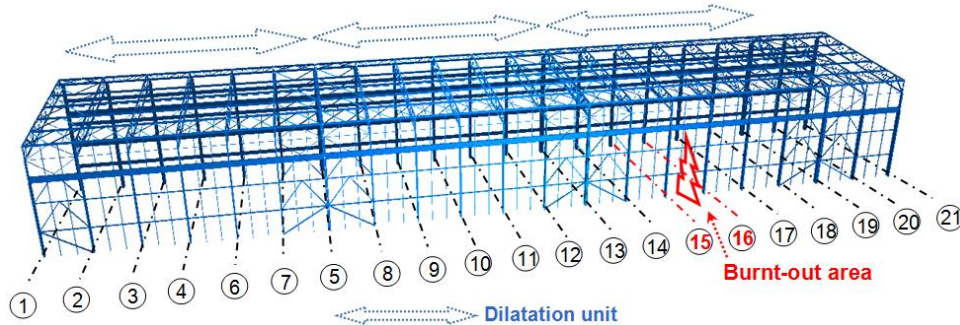


Fig. 1 An axonometric view of the industrial hall with marked axes of the transverse bearing systems and a denotation of the dilatation units and the burnt-out area

procedure that, through the integration of knowledge obtained from complex post-fire inspection, diagnostics, tests and sophisticated computational methods, can improve assessment of residual resistance and serviceability of the structure subjected to the effects of fire.

This paper proposes a methodology and procedure for complex diagnostics and analysis of a damaged industrial hall subjected to the effects of fire. Experimentally obtained current material and geometrical properties create basic input data for theoretical analyses. Responses of the structure obtained numerically are compared with real values. The aim of the paper is to characterize the results of comprehensive failure diagnostics, non-destructive and destructive material tests and detailed static analysis of bearing structures damaged by the effects of fire.

A numerical study of the structural behaviour during the fire was performed to simulate how the temperature affects the resistance of structural members. In order to compare the behaviour of the numerically modelled steel roof truss subjected to the effects of fire with the real post-fire response of the damaged structure; the theoretically obtained resistance, critical temperature and the time at which the structure no longer fulfils the required reliability criteria under its given loading (the structural member lost its load bearing ability and resistance) are compared with real fire condition values.

2. Description of the bearing system of the steel industrial hall

In this paper a steel hall located on the premises of a thermal power plant severely damaged by fire, which broke out at evening is described. Fire-fighters were able to extinguish the fire even at night. The cause of the fire in the thermal power plant was due to a technical problem. A higher operating speed and temperature increase at the start of the fifth thermal power unit caused a fault condition which resulted in the ignition of the cooling oil. The fire subsequently spread via cabled distributions. A fire with a temperature over 800°C for a duration of about 20 min engulfed the full height of the building, and reached the roof structure at a height of 23.7 m. Data on the temperature value were determined by firefighters on the basis of combustion period and a thermo vision camera.

The present industrial building was built and first put into use in 1965. An axonometric view of the industrial hall with marked axes of the transverse bearing systems and a denotation of the dilatation units and the burnt-out area is shown in Fig. 1.

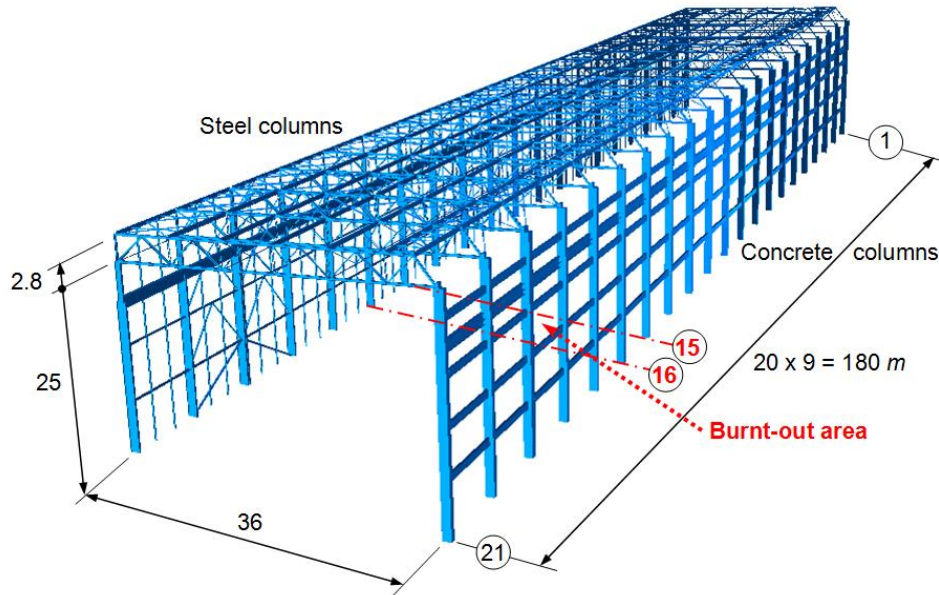


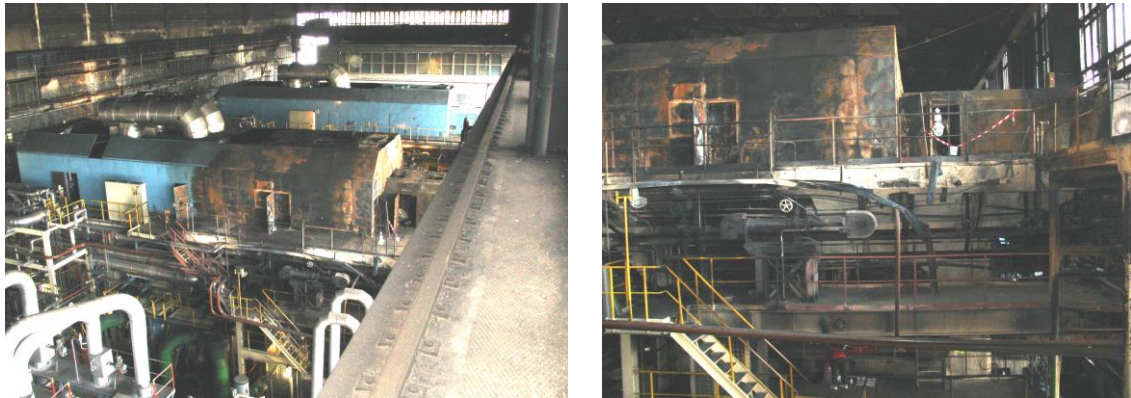
Fig. 2 A scheme of the hall with the basic dimensions and a denotation of the burnt-out area

The span of the hall measures 36.0 m and the length is 180.0 m. A scheme of the hall with basic dimensions is shown in Fig. 2. The bearing system of the single storey industrial building consists of columns made up of welded I-1100 steel sections with transverse stiffeners, situated on the one side of the hall and reinforced concrete columns on the other side (Fig. 2). The distance between the individual columns in the longitudinal direction (longitudinal module) is 9.0 m. The bearing structure of the roof consists of steel planar trusses. Vertical loads acting on the roof are transmitted to the trusses by means of purlins on which lightweight porous concrete panels are located. Roof and wall bracings provide the overall stability of the structure. In the building there is a system of two parallel runways with rails for two bridge cranes with a lifting capacity of 18.0 t. The main girder of the crane runway is made of a welded steel I-1200 section.

3. Post-fire inspection, evaluation of the structure and determination of the extent of damage

The comprehensive diagnostics, tests and static assessment were focused on two basic goals: (i) Detection of the current technical condition of the load bearing structure and the assessment of resistance of their structural members after the fire. (ii) The determination of the degree of damage and the design of reconstruction arrangements which enable the further safe and reliable use of the building.

The results and all information obtained from the non-destructive and destructive tests are used to detect all defects and damage to the structure and subsequently assess the reliability of the steel and concrete structural members and components. The aim is to make such adjustments to all damaged structural members and to take measures in order to ensure the safe use and functionality of the structure.



(a) A fire damaged turbine generator unit

(b) A fire damaged steel members of platforms

Fig. 3 A view of the burnt-out area inside the hall

A view of the burnt-out area inside the hall with a fire damaged turbine generator unit and steel members of platforms damaged by fire are shown in Fig. 3. In general, the effects of fire on the structure and its structural members are characterized by heat expansion and the degradation of mechanical properties of its materials.

3.1 Description of damage

Based on a visual inspection, diagnostics and investigation of the steel structure of the hall the following facts can be introduced:

The main structural members of the roof (concrete panels, purlins, trusses and bracings) and crane runways located in the fire zone between the 15 and 16 axes were subjected to high temperature, approximately 800°C, for a period of twenty minutes, which resulted in excessive deformations of some bearing members. Columns were situated at a distance of approximately 4 m from the burnt-out area.

Plastic deformations of the top chords of the trusses in the 15 and 16 axes and their spatial displacement were identified. The damaged steel roof truss in axis 16 (over the burnt-out area) with the deformed top chord subjected to buckling is shown in Fig. 4(a). The steel material properties start to deteriorate when the temperature exceeds a certain value. When the temperature exceeds a critical value plastic deformations appear at some of structural members. These deformations then expand to the other members over time. The compressed top chord of the truss exhibited a significant flexural deformation which is mainly caused by additional bending moment. This additional bending moment in the top chord is produced by its buckling due to the ex-centric compression force affecting the arm against the original longitudinal axis of the non-deformed member.

The bottom chords of the trusses in the 15 and 16 axes suffered local plastic deformations at the cross-sections near their supports (at the steel columns) as is shown in Fig. 4(b) for the truss in axis 16. This local deformation of the bottom chord is caused by compression due to the restrained elongation (thermal expansion) under elevated temperatures. It is important to mention, that all the joints and connections at the trusses' steel supports were able to resist the reaction forces during the entire fire period.



(a) The deformed top chord of the truss subjected to buckling



(b) The local deformation of the bottom chord of the truss

Fig. 4 Damaged steel roof truss in axis 16 (over the burnt-out area)



Fig. 5 Deformed longitudinal vertical roof bracings at both end parts of the dilatation unit of the hall where the fire was located

A detailed examination of the deformations of the structural members reveals that it is important to highlight the effect of thermal expansion (elongation). Vertical longitudinal roof bracings situated between trusses in the 13 and 14 axes and in the 18 and 19 axes are deformed as

is shown in Fig. 5. These deformed roof bracings are situated at the end parts of the dilatation unit of the hall in which the burnt-out area was identified. Both induced deformations and reaction forces in members located at the ends (supports) of the relevant dilatation unit are caused by compression due to restrained elongations of the bracing members subjected to elevated temperatures (restrained thermal expansions). The side horizontal roof bracings in the roof plane were not deformed.

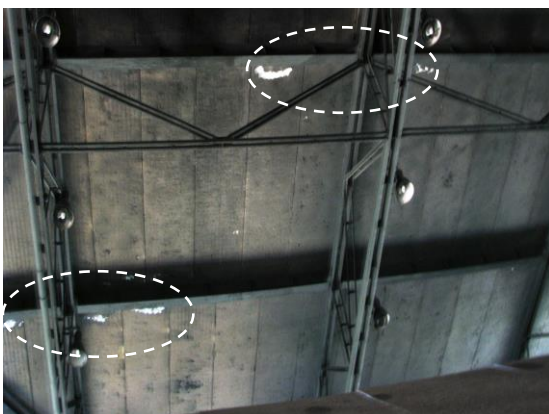
Local web buckling between the transverse stiffeners of the column in the 16 axis was identified. The main girder of the crane track was not distorted.

As a result of elevated temperatures the porous concrete roof panels in the area over the fire zone were damaged. The panels were excessively deflected and deformed. Some of the reinforcement, made of steel rods was subjected to plastic deformation. A bottom view of the roof above the damaged turbo-generator with visibly damaged panels in the anchorage zone and a detail of the damaged panels in the anchorage zone are shown in Fig. 6. During the investigation, initial manufacturing structural imperfections were found. For example, some of the roof panels did not have sufficient concrete cover over the reinforcement; the panels had no shear reinforcement near the supports and had in-sufficient actual lengths of the supports.

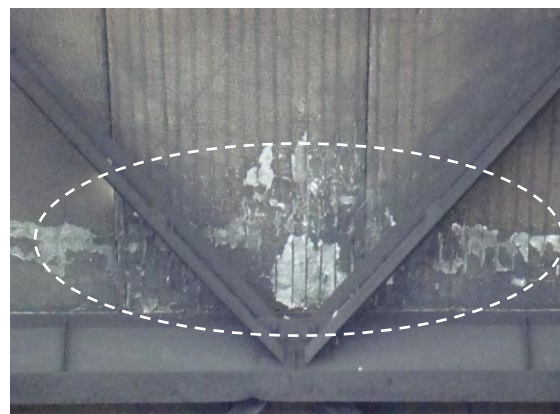
3.2 Non-destructive examination of the structure: inspection and tests in situ

In order to determine the degree and extent of damage of the steel bearing structure after the fire the following non-destructive examinations and investigations of welds and thicknesses of the individual steel member parts were carried out in situ.

- (i) Visual tests were used to identify bad welds after the fire, to reveal possible discontinuities in weld lengths and cracks in welds as well as to obtain important information about the general state of welds in the critical zones of the structure.
- (ii) Magnetic particle tests were used to detect surface defects in welds that are too fine to be seen with the naked eye or that lie slightly below the surface. Welds of the bottom and top chords as well as of the diagonal and vertical members of the trusses (15 and 16), steel columns (16) and the main girder of the crane runway (between the columns 15 and 16) in the critical



(a) Visibly damaged panels in the anchorage zone



(b) A detail of the damaged panels in the anchorage zone

Fig. 6 A bottom view of the roof above the damaged turbo-generator

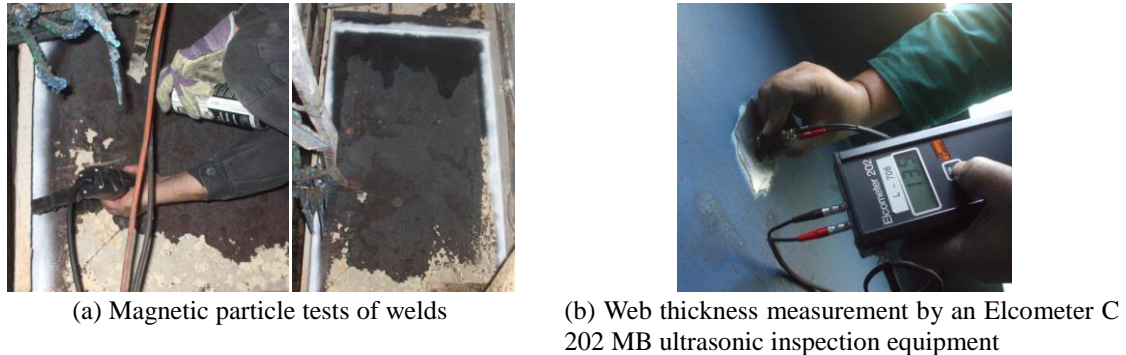


Fig. 7 Inspection of the column in the axis 16

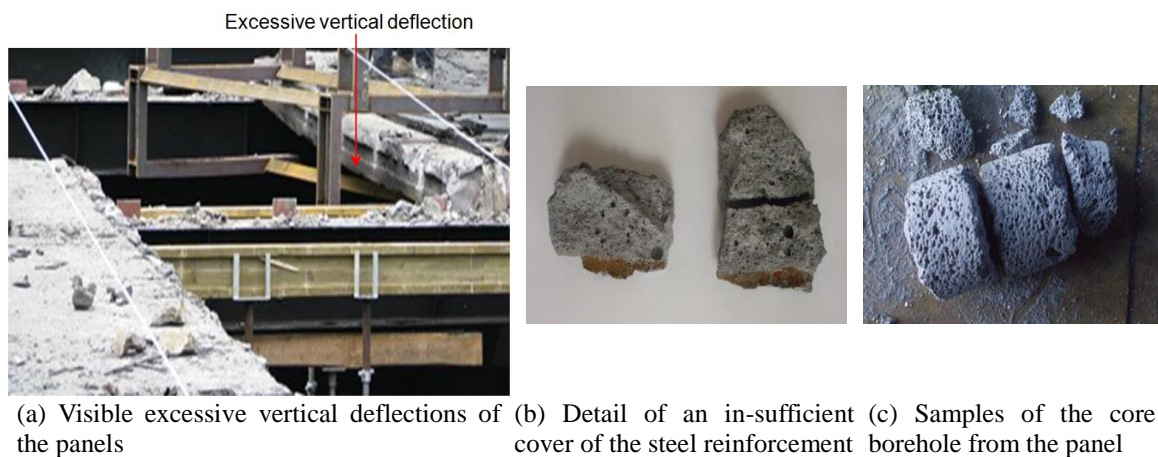


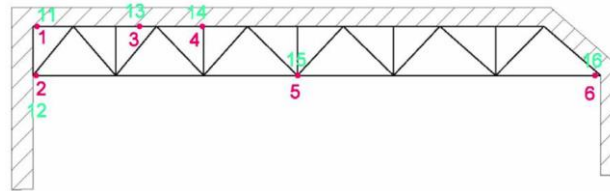
Fig. 8 A current state of the concrete roof panels

zone were tested. Magnetic testing was performed using a Parker/220V magnetizer of a flaw detector. Inspection of the column in axis 16 and magnetic particle tests of welds are shown in Fig. 7(a).

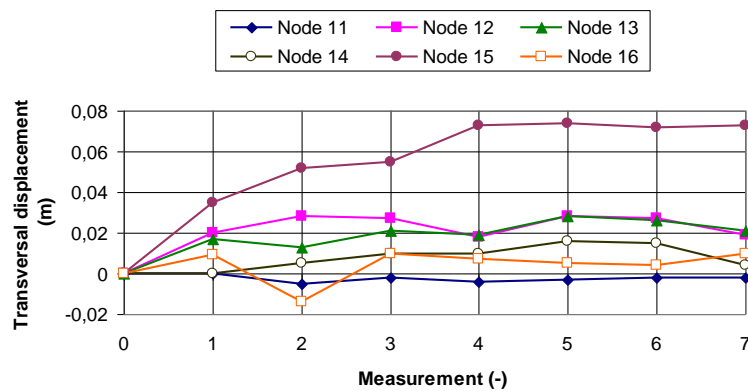
No failures in the welds of the tested members were detected. Visual tests and magnetic particle tests confirmed a general conformity of welds and that their current properties met specifications.

Measurements of the current thicknesses of the cross-sections of the selected members of the steel structure were performed using an Elcometer 204 steel ultrasonic thickness gauge, which provides a fast and accurate measurement of the thickness of steel materials (Fig. 7(b)). Results did not confirm significant deviations from the values stated in the original project documentation.

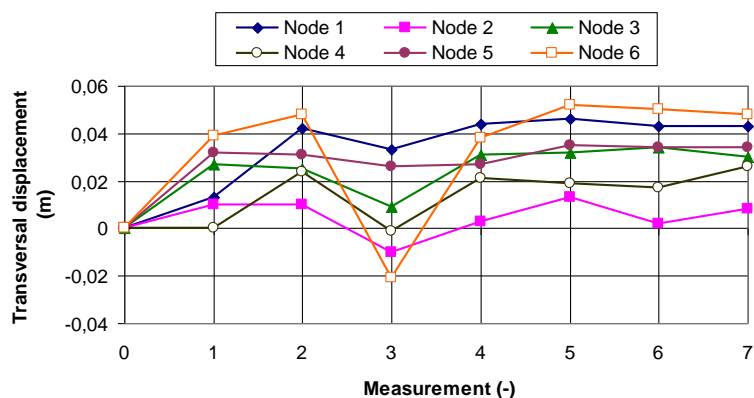
The current state of the concrete roof panels with visible excessive vertical deflections and a detail of in-sufficient cover of the steel reinforcement are shown in Fig. 8(a) and Fig. 8(b). In Fig. 8(b) are panel fragments (photographed in the laboratory with a flash) and in Fig. 8(c) is the borehole from the same panel (photographed directly at the sampling site). The actual strength of the concrete of the roof panel located over the fire area was examined by means of both non-destructive and destructive tests. Based on the tests, analyses and a reliability assessment (a codified verification using partial factors) it was concluded that these concrete roof panels could not be used in the reconstruction process and therefore must be replaced with lightweight roof



(a) A scheme of the denotation of nodes (nodes 11-16 for the truss in the axis 15 and nodes 1-6 for the truss in the axis 16)



(b) Measured displacements of the truss in the axis 15



(c) Measured displacements of the truss in the axis 16

Fig. 9 A geodetic surveying of transversal displacements of selected nodes of the steel roof trusses

sandwich panels created from thin-walled trapezoidal profiles. Another reason for the removal of the concrete panels was an effort to reduce the load imposed on the damaged roof trusses in the critical zone.

3.3 Results of geodetic survey on selected members of the structure

Geodetic measurements of the distorted shape of the steel roof trusses and their deflections as well as a measurement of the rail offset of the crane runway in order to obtain the real geometry of the current post-fire deformed members were performed. The current geometry and actual



(a) A column before and after the collection of specimens with a treatment of the flange after sampling (b) A separation of elements for a generation of specimens for tensile tests

Fig. 10 Preparation of specimens taken from a column

coordinates of the important nodes of the structure is required for further static analyses.

Results obtained by means of a geodetic survey of the transversal displacements of selected nodes of the steel roof trusses are shown in Fig. 9. Continuous geodetic measurements of the selected nodes in the top and bottom chords of the roof trusses in axes 15 and 16 (nodes 11-16 for the truss in axis 15 and nodes 1-6 for the truss in axis 16) confirmed the progressive increase of the displacements (deformations) in the horizontal transversal direction over a period of the four days (Fig. 9). In the place of the buckled chord (truss in the 16 axis) an increment of the displacement in the horizontal direction of approximately 35 mm occurred. In the middle of the bottom chord of the truss in axis 15 the increment of the displacement in the horizontal direction of approximately 76 mm was measured.

The measurements were functions of time, due to structural effects which were connected with a redistribution of forces and influenced by time-dependent changes in a global and local stiffness of the structural system and its deformed members. Progressive plastic deformation of the cross-section in the top chord of the truss occurs and consequently, a redistribution of internal forces between adjacent bars, diagonals, verticals and bracings appeared.

A geodetic survey confirmed that the main girder of the crane runway is not distorted. A displacement of the rail axis obtained by the measurement can be compensated through necessary rectification.

4. Material destructive tests

Material samples were taken from selected steel and concrete structural members (such as the roof trusses and roof bracings, columns, as well as girders of the crane runways and concrete roof panels).

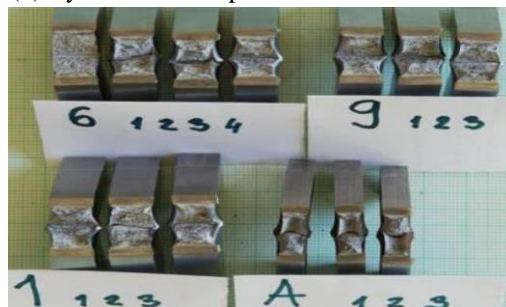
Tests were performed in accredited laboratories at the Technical university of Kosice to determine the current mechanical properties of steel and concrete specimens after the fire. In order to compare the current mechanical properties of steel materials of the structural members, specimens were taken from the following three zones: (i) From the fire zone directly affected by a high temperature (in the burnt-out area between the 15 and 16 axes). (ii) From the zone indirectly affected by the fire (in the vicinity of the fire between the 13, 14 and 15 axes). (iii) From the area unaffected by the fire (between axes 1 to 13).



(a) Flat



(b) Cylindrical test specimens after tensile tests



(c) Broken steel specimens after the Charpy V-notch impact tests

Fig. 11 View of the test specimens

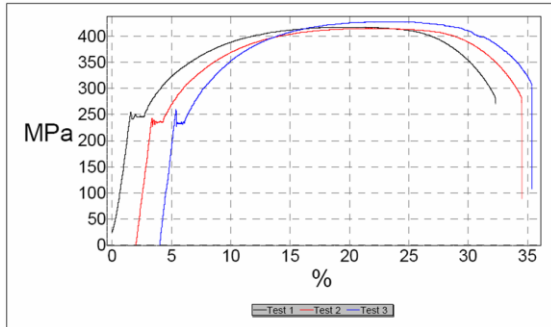
4.1 Results of tensile tests

Tensile tests were conducted on the specimens taken from three different mutually independent zones of the steel structure to obtain and compare their stress-strain curves (diagrams) and relevant mechanical properties such as yield stress f_y (upper and lower yield point), Young's modulus E , ultimate strength f_u and ductility. The amount of elongation at rupture is an important index of material ductility. In total 49 tensile specimens were tested (3 specimens for each sample).

The preparation of specimens taken from a column is illustrated in Fig. 10. Tensile tests were performed on a ZWICK 1387 tensile machine under standardized conditions. A view of the test specimens after the tensile tests is shown in Fig. 11(a) and Fig. 11(b).

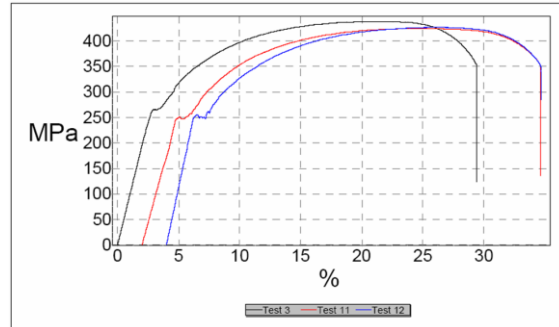
Results of the tensile tests of the steel specimens taken from the horizontal roof bracings in the fire zone (between the 15 and 16 axes) and in the zone near the fire (between the 14 and 15 axes)

name	Spec. No.	Rp0.2 [MPa]	ReH [MPa]	ReL [MPa]	Rm [MPa]
Test 1	1-1	242	254	241	417
Test 2	1-2	238	243	228	415
Test 3	1-3	231	259	230	428



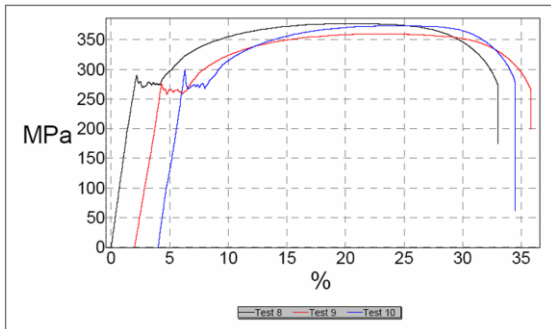
(a) The steel specimens taken from the column in the fire zone (16 axis)

name	Spec. No.	Rp0.2 [MPa]	ReH [MPa]	ReL [MPa]	Rm [MPa]
Test 3	3-1	255	n.a.	n.a.	438
Test 11	3-2	251	251	247	424
Test 12	3-3	255	256	247	426



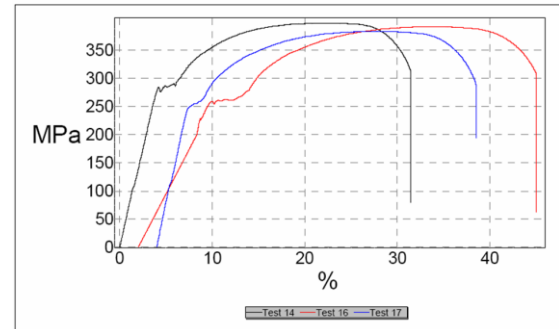
(b) The steel specimens taken from the column in the fire zone (15 axis)

name	Spec. No.	Rp0.2 [MPa]	ReH [MPa]	ReL [MPa]	Rm [MPa]
Test 8	B-1	289	291	269	377
Test 9	B-2	265	276	259	360
Test 10	B-3	280	300	267	374



(c) Steel specimens taken from the horizontal roof bracings in the fire zone (between the 15 and 16 axes)

name	Spec. No.	Rp0.2 [MPa]	ReH [MPa]	ReL [MPa]	Rm [MPa]
Test 14	Z2-1	282	284	276	398
Test 16	Z2-2	118	228	226	392
Test 17	Z2-3	249	n.a.	n.a.	383



(d) Steel specimens taken from the transverse stiffeners of the crane runway beam in the fire zone (between the 15 and 16 axes)

Fig. 12 Typical stress-strain diagrams of tested steels obtained from tensile tests at ambient temperature; with a denotation: $R_{p0.2}=f_{p,0.2}$ is the 0.2 % proof stress, $R_{eH}=f_{y,u}$ is the upper yield point, $R_{eL}=f_{y,l}$ is the lower yield point and $R_m=f_u$ is the ultimate strength

confirmed on average an approximately 10% decrease in the mechanical properties compared to the properties of the specimens taken from the zones unaffected by the fire (between the 7 and 8 axes).

Results of the tensile tests of the steel specimens taken from the columns in the fire zone (15 and 16 axes), in the zone near the fire (13 and 14 axes) and in the zones far-off the fire (6 axis) did not confirm changes of the mechanical properties of the steel.

Results of the tensile tests of the steel specimens taken from the transverse stiffeners of the crane runway beam in the fire zone (between the 15 and 16 axes), confirmed an approximately 10% average decrease of the mechanical properties compared to the properties of the specimens selected from the zones far-off of the fire zone (between the 10-11 and 11-12 axes).

Typical stress-strain diagrams of tested steels obtained from the individual tensile tests at ambient temperature are shown in Fig. 12. All stress-strain curves of the specimens shown in Fig.

12 were taken from fire damaged structural members of the load-bearing structure (e.g., local web buckling of the column, deformations of the horizontal roof bracings) which were directly or indirectly subjected to elevated temperatures and flames. Specimens were not taken from the structural members of the truss affected by plastic deformations (Fig. 4) by reason of preservation of structural integrity for further use after strengthening. These stress-strain curves were compared with curves obtained for the specimens taken from the zones unaffected by the fire.

Tensile diagrams correspond to the low carbon structural steel used for welded structures. The fracture appearance of tested specimens corresponds to their mechanical properties for structural steel. No anomalies in the behaviour of tested samples were detected.

Regarding the tensile tests, specimens taken from the horizontal roof bracings (Fig. 12(c)) and from the transverse stiffeners of the crane runway beam (Fig. 12(d)) in the fire zone showed a 10 % decrease in mechanical properties (yield strength and ultimate strength) compared to the properties of the specimens taken from the zones unaffected by the fire, while other specimens taken from the columns (Fig. 12(a) and Fig. 12(b)) in the fire zone (15 and 16 axes), did not show significant decreases. This can be explained as follows. Columns were situated at a distance of approximately 4 m from the burnt-out area which was about 6 m above the floor, at the place where the turbine generator unit was located. Thus, the columns were not exposed to direct flame in contrast to the horizontal roof bracings, which were closest to the fire, and were directly exposed to flames. This was also confirmed by the results of analyzes. Calculations showed that the columns were not subjected to a temperature of 800 °C after 20 minutes of fire effects but only to 427°C.

For Young's modulus a special ZWICK 7852 extensometer with a high accuracy was used (Fig. 13(a)). Stress-strain diagrams for the determination of Young's modulus for selected steel specimens are shown in Fig. 13(b). Three specimens for each variable were tested. The Young's modulus was calculated from the initial slope of the stress-strain curve. The Young's modulus remained relatively unchanged for the given steel. The steel revealed an approximately 4% reduction in Young's modulus due to elevated temperatures.

Although the values of steel properties at elevated temperatures are given in the literature (Eurocode), the properties of the heated material after cooling are not available. Consequently, it is not possible to compare the material test results with existing literature concerning temperature dependent material properties of steel and see if the results are reasonable.

4.2 Results of Charpy V-notch impact tests

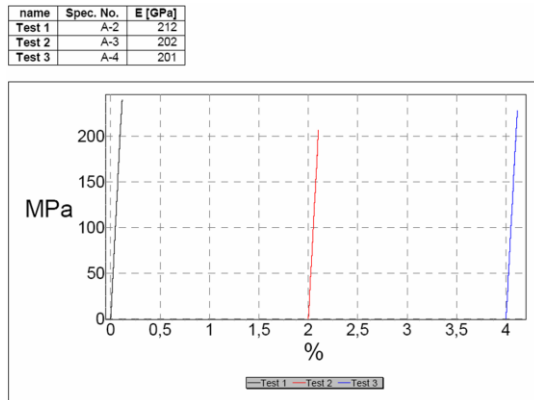
It is in the nature of all materials to contain some imperfections and accidental properties. In steel these imperfections take the form of very small cracks. If the steel is insufficiently tough, the crack can propagate rapidly, without plastic deformation and results in a brittle fracture. The risk of brittle fracture increases with thickness, tensile stress, stress raisers and at lower temperatures. The toughness of steel and its ability to resist brittle fracture are dependent on a number of factors that should be considered at the specification stage. A convenient measure of toughness is the Charpy V-notch impact test.

Toughness test gives a measure of the resistance of the material against brittle fracture. It is well known that toughness values depend on specimen shape, which varies according to the different standard methods of testing (Charpy V, Mesnager, DVN, etc.), as brittle rupture is influenced by them (Ballio and Mazzolani 1983).

Results of Charpy V-notch impact tests of the steel specimens taken from the column in the fire

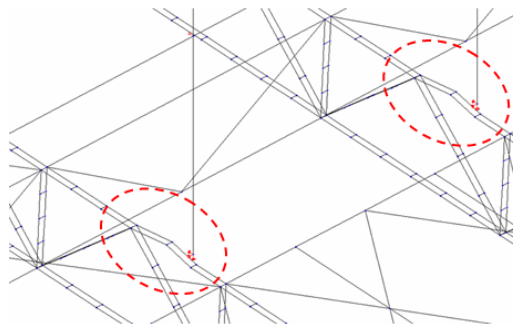


(a) A strain sensor ZWICK 7852 extensometer for measuring the Young's modulus

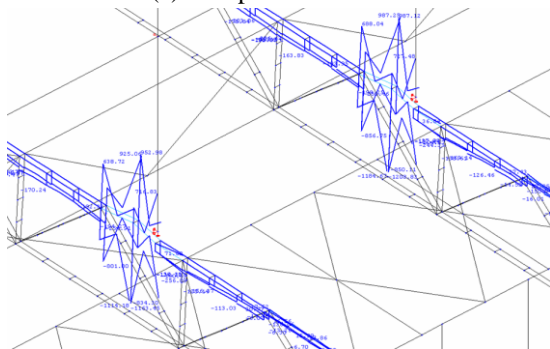


(b) Stress-strain diagrams for the determination of Young's modulus for the specimens taken from the horizontal roof bracings in the fire zone (between the 15 and 16 axes) at a height of 23.7 m

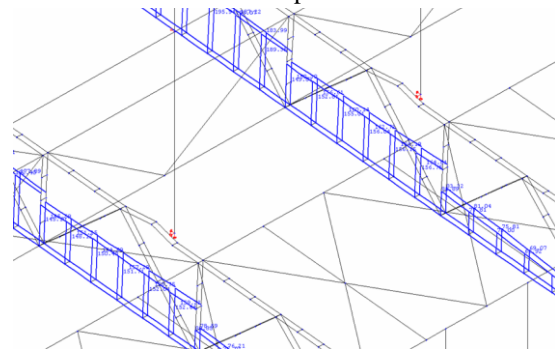
Fig. 13 Determination of the current Young's modulus E



(a) Computational models of the trusses with the introduction of imperfections



(b) Resultant distributions of stresses in the top



(c) Bottom chords of the trusses

Fig. 14 Analysis of the damaged structure with current properties

zone (16 axis) did not confirm a decrease of toughness. A view of the broken steel specimens after the Charpy V-notch impact tests is shown in Fig. 11(c).

Results of Charpy V-notch toughness tests of the steel specimens taken from the roof horizontal

bracing in the fire zone (between 15 and 16 axes) did not confirm a decrease in toughness.

5. Analysis of the post-fire behaviour of the steel structure

The basic prerequisite for a realistic static assessment of the industrial hall damaged by fire is the knowledge of the current state of physical properties of the individual structural members as well as the function of their static behaviour in the load bearing system. The current parameters must be implemented into an adequate computational model of the damaged structure in order to achieve an optimal accordance between the real behaviour of the structure and the theoretically simulated response obtained by the static computational model.

The structure was designed in 1964 according to applicable standards of that time. From the original project documentation it was not possible to determine the steel grade. The current mechanical properties of the steel material (yield stress, ultimate tensile strength and Young's modulus) obtained from the tests and real measured geometric characteristics of structural members with imperfections were used for the creation of computational models and subsequent static analyses.

The determination of the applied load and the assessment of the reliability of the damaged structure in its current state were performed according to current standards. The behaviour of the steel structure after the fire is investigated numerically to verify the adequacy of steel members exposed to the fire.

5.1 Computational models and static analysis

The finite element method was used to study the post-fire behaviour of the structure. Geometrically nonlinear analyses were conducted using Scia Engineer software (Scia Engineer 2013). The three-dimensional spatial finite element model of the bearing system of the structure consisted of 2 423 nodes and 3 952 elements.

An assessment of the steel structure and its structural members subjected to a minimum load at the current state was performed, hence only the effect of a dead load was considered. In the analysis of the roof trusses the following loads were considered: The permanent load consisting of the self-weight of the steel structure (directly generated in a computer program) and of the roof panels with cladding (self-weight of lightweight porous concrete panels 1.574 kNm^{-2} and insulation layers of the roof cladding 0.42 kNm^{-2}).

Two models of imperfection were taken into account during the analyses. The deviation of the top chord of the trusses from the straight axis in the longitudinal direction and an interruption of the top chord of the trusses (in the place of deviation of the top chord) were considered in the computational models of the steel structure of the hall.

5.2 Results of the static analyses

For the analysis and reliability assessment of the damaged structure with current properties a deviation of the top chords of the trusses in the fire zone (between the 15 and 16 axes) with a size of 200 mm was considered (Fig. 4(a)). Computational models of the trusses with the introduction of imperfections as well as resultant distributions of stresses in the top and bottom chords of the trusses are shown in Fig. 14. Results of the static analysis confirmed that the stresses in the top

chords of the trusses (in the areas of considered imperfections) are beyond the elastic limit and chords are characterized by a plastic behaviour (Fig. 14(b)).

The maximum vertical deflection obtained from the analysis of the trusses with imperfections subjected to their self-weight and the weight of the roof panels with cladding is 137 mm. As load redistribution is highly efficient within the steel trusses owing to their effective structural forms; the failure of any member does not necessarily signify a whole system failure.

Thus, it is appropriate to assess the system failure of steel trusses against a global deflection limit of $w_{lim}=l/250=36000/250=144$ mm. Thus it can be seen that the deflection of the truss subjected to its self-weight and weight of the roof panels with cladding almost reaches the allowable limit value of the global deflection of the truss subjected to the total load consisting of the permanent and variable loading parts. This methodology only refers to the current state of the truss subjected solely to the permanent load when the criterion of serviceability limit states was already reached.

For validation of the analysis, the maximum vertical deflection obtained from the analysis of the truss was compared with the geodetic surveying of transversal displacements (Fig. 9). The maximum vertical deflection at the middle of the truss obtained from the analysis is $w=137$ mm and the maximum increment of the transversal displacement at the same place obtained by the geodetic surveying is $v_i=76$ mm.

The total transversal displacement is $v=v_0+v_i=57+76=133$ mm, because $v_0=57$ mm is the initial displacement after the fire. Results showed that individual values are comparable, so that confirmed a physical relevance and mathematical correctness of the applied theoretical approach.

Computational models of the trusses with intermittent top chords in the damaged areas and resultant distributions of stresses in the top and bottom chords of the trusses are shown in Fig. 15. An analysis of the diminished structure with the current properties confirmed that the edge bars of the bottom chords near supports are subjected to compression which correspond to the real damage of the bottom chord of the truss as is revealed in Fig. 4(b).

Results of the geometrically nonlinear static analyses of the steel structure with the current properties and substantial conclusions from the assessment of its reliability can be briefly summarized as follows:

The current behaviour of the roof trusses located between the 15 and 16 axes (location area of the fire) exceeds the limits of the allowable stresses and deflections. Consequently, the roof trusses do not fulfil reliability criteria defined by the ultimate limit states and serviceability limit states.

The columns fulfil reliability conditions in this case, providing that the locally damaged (buckled) web of the column in the 16 axis be reinforced.

6. Temporary safety measures and implementation of the renewal

Based on diagnostics, investigations, tests and numerical analyses the following safety measures were undertaken: Temporary protection of the damaged structural members, removal of the concrete roof panels from the relevant area in order to unburden the damaged roof trusses and subsequent reconstruction of the hall.

In accordance with those provisions a stabilization and unburdening of the roof trusses in the 15 and 16 axes by means of the placement of temporary supporting struts under the purlins in the areas between the 14-15, 15-16 and 16-17 axes were performed. These provisional arrangements helped achieve the required reliability of the roof structure during the subsequent reconstruction. A

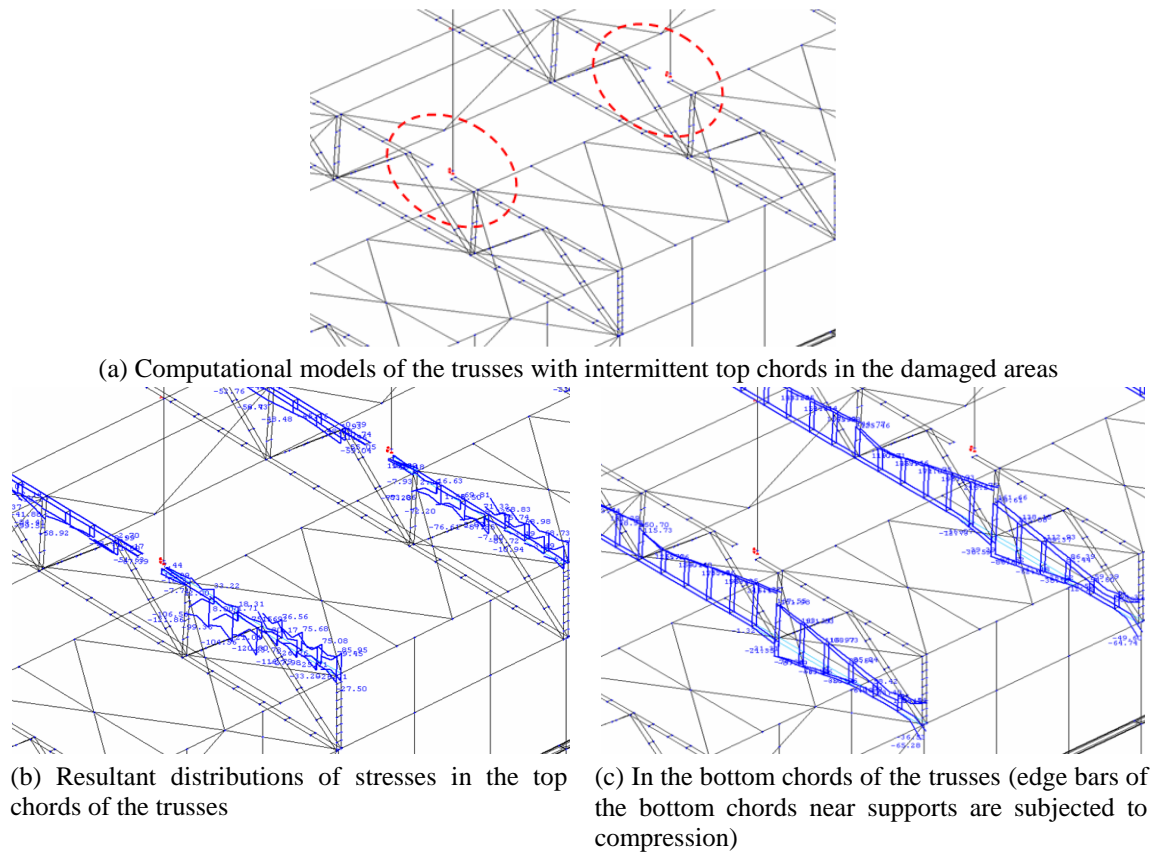
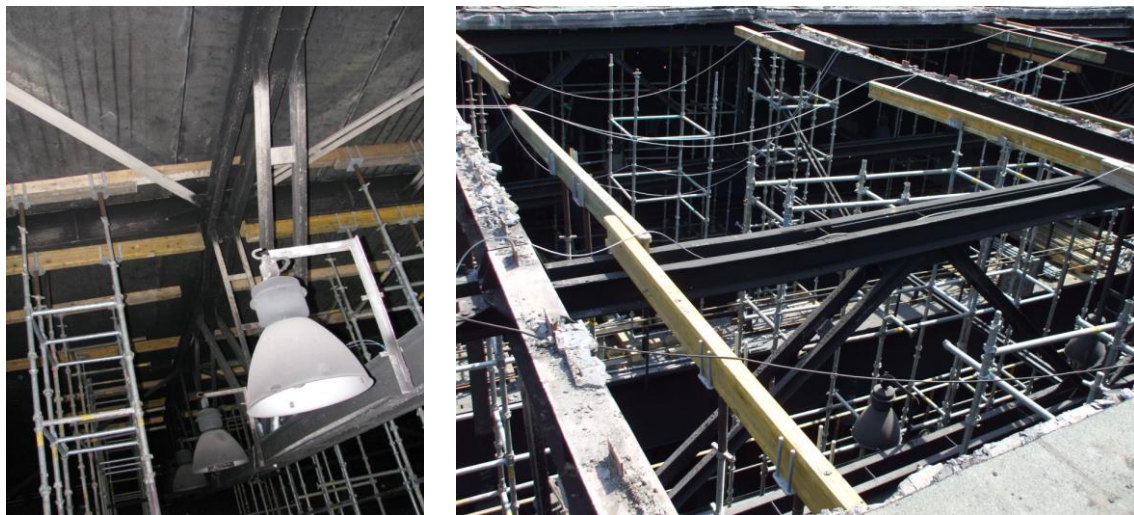


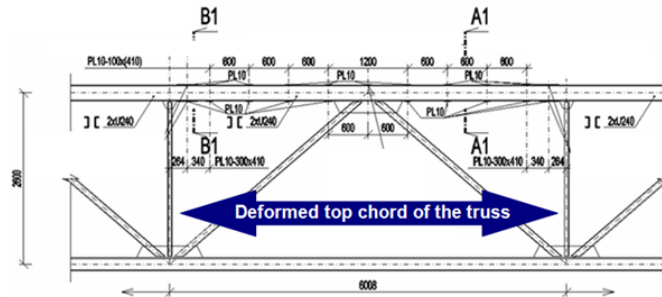
Fig. 15 Analysis of the damaged structure with the current properties



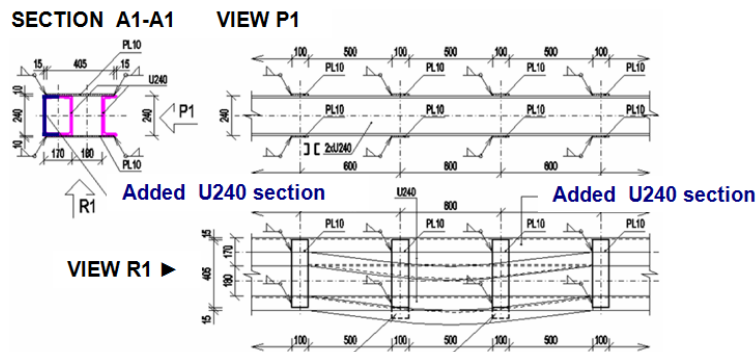
(a) Purlins supported by struts stored on the cranes (b) View of the roof structure after the removal of the concrete roof panels

Fig. 16 Reconstruction of the roof structure of the hall

STRENGTHENING OF THE TRUSS



(a) Deformed top chord of the truss



(b) A scheme of the strengthening



(c) The strengthened truss with the new light-weight sandwich roof cladding after the reconstruction

Fig. 17 Strengthening of the steel truss

temporary supporting system with damping members was placed on the bridge cranes. The top chords of the trusses were stabilized by brace struts at the nodes of the trusses in the places of deviations. After removing the porous concrete roof panels between the 14-15, 15-16 and 16-17 axes, the necessary strengthening of the top chords of the trusses was carried out. Reconstruction of the roof structure of the hall, the purlins supported by struts stored on the cranes and a view of the roof structure after the removal of the concrete roof panels are shown in Fig. 16. The concrete panels were replaced with a light-weight sandwich roof cladding. The steel truss with the deformed top chord was strengthened. A scheme of the strengthening and the strengthened truss

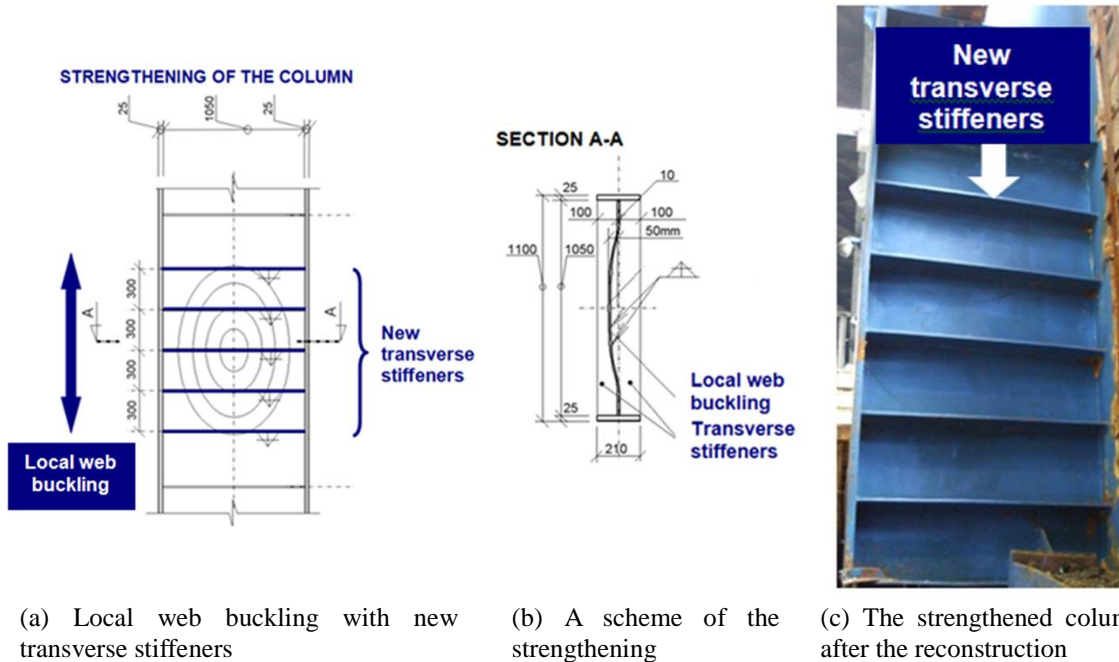


Fig. 18 Strengthening of the steel column

with the new light-weight sandwich roof cladding after the reconstruction is shown in Fig. 17.

Locally deformed bottom chords of the trusses were strengthened by means of additional steel sheets around the cross-section which enables the creation of a hollow section.

Strengthening a locally failed web of the column in the 16 axis by the addition of transverse stiffeners was performed (Fig. 18(a) and Fig. 18(b)). The strengthened column after the reconstruction is shown in Fig. 18(c).

7. Analysis of the steel structure subjected to fire

In this section the expected behaviour of the steel structure and its structural members under relevant fire conditions is simulated. The computational model can provide a realistic analysis of the structure exposed to fire.

The finite element method is applied to simulate the behaviour of the investigated steel structure subjected to the effects of fire. Finite element Scia Engineer software was used for the modelling and time-dependent fire resistance analyses (Scia Engineer 2013).

The four basic steps of modelling required for the analysis of the behaviour of the steel structure subjected to fire are: a structural model, material properties model, fire model and heat transfer model.

For the analysis of the structure subjected to temperature effects during a fire any of the following methods can be used: global analysis of the structure; analysis of part of the structure or analysis of the structural member.

7.1 Mechanical properties of steels subjected to elevated temperatures

Fire resistance of the steel structures is determined according to EN 1993-1-2 (Eurocode 3 2005) and related standards. Fire resistance is expressed as the time for which preservation of the stability and resistance of the structure and its structural members is guaranteed. The intense heating of a steel structural member and the decrease of its material characteristics occurs during the fire. If the decrease of yield stress is high, the structural member can deform or break. The temperature at which deformation and/or break occurs, is the critical temperature. This temperature is achieved for usual types of structural steels at approximately 550°C, but may also be different depending on the dimensions of a structural member. At this temperature the steel maintains only about 60% of the initial yield stress, compared with normal temperature.

Design values of mechanical steel properties (strength and deformation) $X_{d,fi}$ at elevated temperatures are defined as (Eurocode 3 2005)

$$X_{d,fi} = \frac{k_{\theta} X_k}{\gamma_{M,fi}} \quad (1)$$

where X_k is the characteristic value of a strength or Young's modulus for normal temperature design, k_{θ} is the reduction factor for a strength or deformation property ($X_{k,\theta} / X_k$), dependent on the steel temperature and $\gamma_{M,fi}$ is the partial factor for the relevant material property and for the fire situation.

The steel properties depend on the temperature. Reduction factors for steel strength and stiffness at elevated temperatures are defined as follows (Eurocode 3 2005):

Reduction factor for the effective yield strength relative to yield strength at 20°C

$$k_{y,\theta} = \frac{f_{y,\theta}}{f_y} \quad (2)$$

Reduction factor for the proportional limit relative to yield strength at 20°C

$$k_{p,\theta} = \frac{f_{p,\theta}}{f_y} \quad (3)$$

Reduction factor for the slope of linear elastic range relative to slope at 20°C

$$k_{E,\theta} = \frac{E_{a,\theta}}{E_a} \quad (4)$$

The variation of these reduction factors with temperature is illustrated in Fig. 19.

7.2 Temperature-time curve and steel temperature development

In the numerical simulation of the structure and/or structural member the nominal ISO 834 temperature-time curve describing the effect of the fire was considered. The temperature-time curve takes the form (Eurocode 1 2002)

$$\theta_g = 20 + 345 \log_{10}(8t + 1) \quad (5)$$

where θ_g is the gas temperature in °C and t is the time in min. A nominal curve is used for

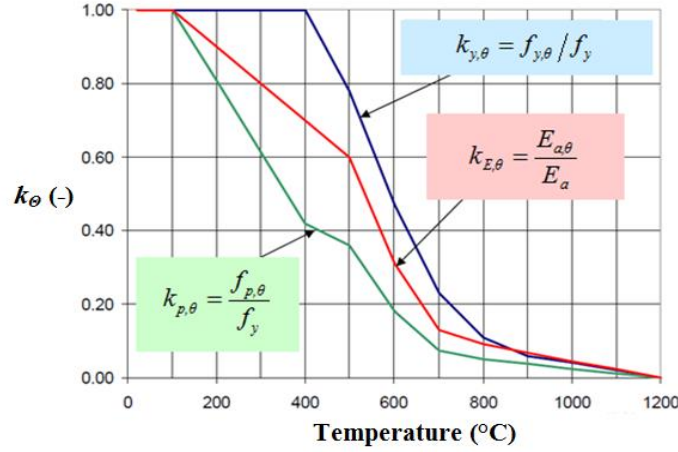


Fig. 19 Reduction factors of the material characteristics of the steel at elevated temperatures

representing a model of a fully developed fire in a compartment. Considering the fire resistance of members subjected to an ISO fire is not at all the same as the fire resistance of members subjected to a natural fire.

The temperature was assumed to be acting on all sides of the individual members of the structure and the fireproof coating was not considered. The increase of temperature $\Delta\theta_{a,t}$ in an unprotected steel member during a time interval Δt can be written as

$$\Delta\theta_{a,t} = k_{sh} \frac{A_m}{c_a \rho_a} h_{net,d} \Delta t \quad (6)$$

where A_m is the exposed surface area per unit length, V is the volume of the member per unit length, k_{sh} is the correction factor for the shadow effect, c_a is the specific heat of steel, ρ_a is the unit mass of steel, $h_{net,d}$ is the net heat flux per unit area and Δt is the time interval in seconds.

The fire model was represented by an ISO 834 temperature-time curve together with heat transfer model in the form of the net heat flux $h_{net,d}$

$$h_{net,d} = \gamma_{n,c} h_{net,c} + \gamma_{n,r} h_{net,r} \quad (7)$$

which was used in expression (6) for the increase of temperature in the unprotected steel member. In expression (7) $h_{net,c}$ is the convective heat flux, $h_{net,r}$ is the radiative heat flux, $\gamma_{n,c}$ and $\gamma_{n,r}$ are factors for the convective and radiative heat flux, respectively. The convective heat flux $h_{net,c}$ is calculated as

$$h_{net,c} = \alpha_c (\theta_g - \theta_m) \quad (8)$$

where α_c is the coefficient of the heat transfer by convection, θ_g is the gas temperature in °C and θ_m is the surface temperature of the structural member in °C. The radiative heat flux $h_{net,r}$ can be written in the form

$$h_{net,r} = \Phi \cdot \varepsilon_{res} \cdot 5.67 \cdot 10^{-3} \left((\theta_r + 273)^4 - (\theta_m + 273)^4 \right) \quad (9)$$

where Φ is the configuration factor, ε_{res} is the resultant emissivity and $\theta_r = \theta_g$ is the gas temperature in °C.

Two types of analysis were performed: the fire resistance check in the resistance or strength domain and temperature / time domain. In both analyses the above mentioned fire model and heat transfer model were applied contemporaneously.

In the resistance domain the unprotected structure was subjected to permanent load and fire action with a duration of 20 minutes. During the calculation, values of yield strength and Young's modulus are reduced depending on the current temperature and the resistance of the individual structural members is assessed. In this approach, a coupled heat transfer and structural analysis, such that the deformations of the structure were calculated based on thermal expansion as well as mechanical loading was used.

In the temperature / time domain the unprotected structure was subjected to permanent load and fire action and the time when the temperature of the structural member was higher than the critical temperature of the member material was calculated. The material temperature is checked in relation to the critical material temperature.

Both computational approaches confirmed the loss of resistance of the structure affected by the fire after approximately 20 minutes.

7.3 Results and discussion

In order to compare the behaviour of the numerically modelled steel roof truss subjected to the effects of fire with the real post-fire response of the damaged structure the theoretically obtained resistance, critical temperature and the time at which the structure no longer meets the reliability criteria under its given loading (the structural member lost its load bearing ability and resistance) are compared with the real values subjected to fire conditions.

The assessment of fire resistance of the steel truss in axis 16 (over the burnt-out area) was performed in the resistance domain and in the temperature-time domain.

In the resistance domain, the resistance of the truss and its members subjected to a temperature exposure is checked after the imposed time. Resistance of the individual members of the steel truss subjected to the fire effects depending on the time, where the members with the unsatisfactory resistance at the individual times are marked is shown in Fig. 20. Resistance of the structure decreases with time due to a decrease of the relevant values of the material properties of the steel subjected to elevated temperatures.

It should be noted, that the applied stresses in all the marked members of the steel truss (Fig. 20) are larger than the design strengths of steel at the corresponding temperatures. A structural member of the truss is considered to fail when the applied stress of the member σ is greater than the design value of strength at corresponding elevated temperature $f_{d,fi}$ which can be written as

$$\sigma > f_{d,fi} = \frac{k_{y,\theta} f_y}{\gamma_{M,fi}} \quad (10)$$

where f_y is the characteristic value of the yield strength for the normal temperature design, $k_{y,\theta}$ is the reduction factor for the yield strength, dependent on the steel temperature and $\gamma_{M,fi}$ is the partial reliability factor.

In the temperature-time domain, the material temperature after fire exposure is checked in relation to the critical temperature of the material. The critical temperature of a member is the

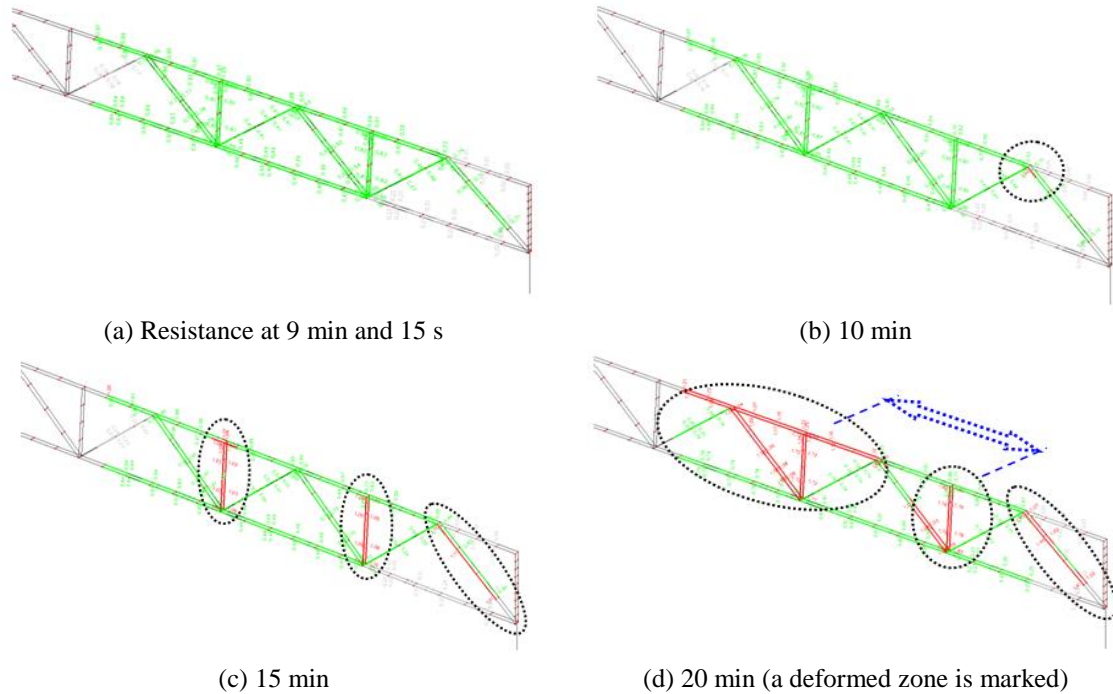


Fig. 20 Resistance of the individual members of the steel truss subjected to the fire effects depending on the time, where the members with the unsatisfactory resistance are marked

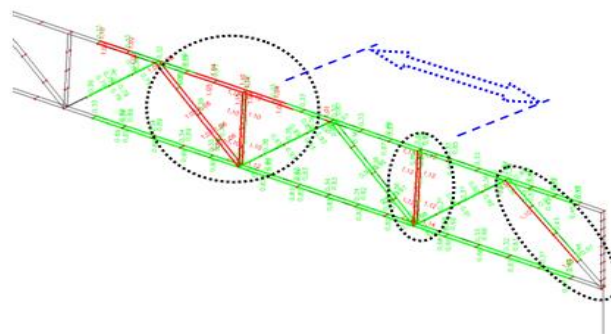


Fig. 21 Assessment of the individual members of the steel truss subjected to the effects of fire in the temperature-time domain with the marked members which reached temperatures higher than the critical temperature over a period of 20 min (a deformed zone is marked)

temperature at which the isolated member in fire conditions under consideration will no longer meet the required criteria under its given loading.

The assessment of the individual members of the steel truss subjected to fire effects in the temperature-time domain with marked members reached temperatures higher than the critical temperature over a period of 20 min is shown in Fig. 21 (a deformed zone is marked). The critical temperature was identified for each structural member by means of an iterative process.

The results obtained by finite element analyses in both the resistance and temperature-time

domain are identical with those observed on the behaviour of the real steel roof truss subjected to the fire effects. Buckling of the top chord of the truss (Fig. 4(a), Fig. 20(d) and Fig. 21) confirms the correctness of computational models and accuracy of numerical analyses used in this study. The time during which the direct flame intensity affected the truss in real fire conditions was approximately 20 min and consequently the truss was deformed. The maximum temperature at which the truss is no longer able to meet the required reliability criteria obtained by means of the numerical simulation is $\theta=781^{\circ}\text{C}$ which occurs 20 min after ignition. A very good agreement between the real characteristics of the structure after fire and simulated results was observed.

8. Conclusions

An analysis and assessment of the reliability of the structure after a fire belong to demanding engineering tasks. These are based on the survey and diagnostics of the current state of the structure affected by the fire and on the experimental verification together with the numerical modelling of the corresponding material, geometric and stiffness properties of the structure and its static analysis. Currently available sophisticated software products based on advanced numerical methods, allow for complex modelling of properties of structures subjected to the effects of various physical fields, which exponentiate a realistic characterization and simulation of their behaviour under defined conditions.

Results of the comprehensive failure diagnostics, non-destructive and destructive tests of steel and concrete materials, geodetic surveying of selected members of the structure, numerical modelling, static analysis and reliability assessment of the load bearing structures of the industrial hall severely damaged by fire effects were presented in the paper. The results demonstrated that the behaviour of the structure subjected to the effects of fire can be closely simulated theoretically (numerically).

Based on the experimentally and theoretically obtained results suitable safety measures were undertaken and the required reliability of the load bearing structure of the industrial hall was once again achieved.

An appropriate evaluation of fire effects for designing durable and safe structures requires the application of reliable experimental methods for investigation current material characteristics (a material properties problem), and for determining the consequent response of structures with an adequate degree of accuracy (a structural analysis problem).

The proposed approach can be used for these purposes since it provides complex analysis of behaviour of structures after fire. The procedure provides the designer with effective ways of guiding the reconstruction of the load-bearing system by an appropriate and rational choice of its parameters.

Acknowledgments

This work is part of Research Project No. 1/0302/16, partially founded by the Scientific Grant Agency of the Ministry of Education of Slovak Republic and the Slovak Academy of Sciences. The present research has been carried out within the project Centre of excellent integrated research for progressive building structures, materials and technologies, supported by European Union Structural funds.

References

- Aslani, F. and Bastami, M. (2011), "Constitutive relationships for normal- and high-strength concrete at elevated temperatures", *ACI Mater. J.*, **108**(4), 355-364.
- Aslani, F. and Samali, B. (2013), "Predicting the bond between concrete and reinforcing steel at elevated temperatures", *Struct. Eng. Mech.*, **48**(5), 643-660.
- Bailey, C.G. (2004), "Membrane action of slab/beam composite floor systems in fire", *Eng. Struct.*, **26**(12), 1691-1703.
- Ballio, G. and Mazzolani, F.M. (1983), *Theory and design of steel structures*, Chapman and Hall, New York, NY, USA.
- Brandt, T., Varma, A., Rankin, B., Marcu, S., Connor, R. and Harries, K. (2011), *Effects of fire damage on the structural properties of steel bridge elements*, University of Pittsburgh, Pittsburgh, USA.
- Chen, Ch.K. and Zhang, W. (2011), "Experimental study of the mechanical behaviour of steel staggered truss system under pool fire conditions", *Thin Wall. Struct.*, **49**, 1442-1451.
- Choi, J., Haj-Ali, R. and Kim, H.S. (2012), "Integrated fire dynamic and thermomechanical modeling of a bridge under fire", *Struct. Eng. Mech.*, **42**(6), 815-829.
- Eurocode 3 (2005), *EN-1993-1-2: 2005*, Design of steel structures, Part 1-2: General rules-Structural fire design, Brussels.
- Eurocode 1 (2002), *EN-1991-1-2: 2002*, Actions on structures, Part 1-2: General actions-Actions on structures exposed to fire, Brussels.
- Foster, S., Chladna, M., Hsieh, C., Burgess, I. and Plank, R. (2007), "Thermal and structural behaviour of a full-scale composite building subject to a severe compartment fire", *Fire Saf. J.*, **42**(3), 183-199.
- Gunalan, S. and Mahendran, M. (2014), "Post-fire mechanical properties of cold-formed steels", *Eurosteel 2014*, Naples, Italy, September.
- He, S.B., Shao, Y.B., Zhang, H.Y., Yang, D.P. and Long, F.L. (2013), "Experimental study on circular hollow section (CHS) tubular K-joints at elevated temperature", *Eng. Fail. Anal.*, **34**, 204-216.
- Ho, H.C., Chung, K.F. and Wong, Y. (2011), "Structural fire engineering study on unprotected long span steel trusses", *Procedia Eng.*, **14**, 1132-1139.
- JalaliLarijani, R., Celikag, M., Aghayan, I. and Kazemi, M. (2013), "Progressive collapse analysis of two existing steel buildings using a linear static procedure", *Struct. Eng. Mech.*, **48**(2), 207-220.
- Jin, M., Zhao, J., Liu, M. and Chang, J. (2011), "Parametric analysis of mechanical behaviour of steel planar tubular truss under fire", *J. Constr. Steel Res.*, **67**(1), 75-83.
- Krentowski, J. (2015), "Disaster of an industrial hall caused by an explosion of wood dust and fire", *Eng. Fail. Anal.*, **56**, 403-411.
- Olmati, P., Petrini, F. and Bontempi, F. (2013), "Numerical analyses for the structural assessment of steel buildings under explosions", *Struct. Eng. Mech.*, **45**(6), 803-819.
- Ozyurt, E. and Wang, Y.C. (2015), "Effects of truss behaviour on critical temperatures of welded steel tubular truss members exposed to uniform fire", *Eng. Struct.*, **88**, 225-240.
- Scia Engineer (2013), *Scia Engineer manuals*, Nemetschek Scia, Nemetschek Vectorworks, Columbia, MD, USA.
- Wald, F., Simoes da Silva, L., Moore, D.B., Lennon, T., Chladna, M., Santiago, A., Benes, M. and Borges, L. (2006), "Experimental behaviour of a steel structure under natural fire", *Fire Saf. J.*, **41**(7), 509-522.
- Wald, F., Sokol, Z. and Moore, D. (2009), "Horizontal forces in steel structures tested in fire", *J. Constr. Steel Res.*, **65**(8-9), 1896-1903.
- Whelan, M., Tempest, B. and Scott, D. (2005), "Post-fire nondestructive evaluation of a prestressed concrete double-tee joist roof", *J. Perform. Constr. Facil.*, **29**(2), 04014055.